Pergamon

Int. J. Solids Structures Vol. 34, No. 6, pp. 703–726, 1997

0020–7683/97 $17.00 + .00

PII: S0020–7683(96)00051–0

INFLUENCE OF MICROSTRUCTURAL VARIATIONS ON STEADY STATE CREEP AND FACET STRESSES IN 2-D FREELY SLIDING POLYCRYSTALS

PATRICK ONCK and ERIK VAN DER GIESSEN
Delft University of Technology, Laboratory for Engineering Mechanics, P.O. Box 5033, 2600 GA Delft, The Netherlands

(*Received* 31 *October* 1995; *in revised form* 13 *March* 1996)

Abstract—At elevated temperatures, creep in polycrystalline aggregates is often accompanied by free grain boundary sliding, which tends to enhance the macroscopic creep rate and the transverse facet stresses. This paper deals with the influence on these phenomena of variations in the microstructure, in terms of variations in the size and shape of grains in an aggregate. Numerical results for two-dimensional cell analyses involving many grains are presented which demonstrate that random microstructural variations relative to an array of regular hexagonal grains invariably lead to an increase of the creep rate enhancement due to sliding. For power-law creeping grains and for the variations considered here, the effects amount to up to a 60% increase. Moreover, it is shown that microstructural variations lead to a wider distribution of transverse facet stress levels with a considerably higher average than for regular hexagonal grains. Both effects are of significance for creep rupture life time estimates. Copyright © 1997 Elsevier Science Ltd.

1. INTRODUCTION

At elevated temperatures and typical creep loading conditions, creep in polycrystalline engineering metals is often accompanied by grain boundary sliding. This is due to the fact that the resistance of grain boundaries against sliding of the adjacent grains relative to each other is low compared to the creep resistance of the grains themselves. Even though irregularities of the grain boundaries, such as ledges, and second-phase particles act as barriers for grain boundary sliding, the sliding resistance in many materials is frequently considered to be negligible all together (see, e.g., Ashby, 1972).

In such cases of completely free grain boundary sliding, the overall creep rate of the polycrystalline material is increased appreciably compared to that in the absence of grain boundary sliding. There has been substantial interest in linking the overall (macroscopic) creep response to that of the (microscopic) response of the constituting grains for over two decades. Assuming simple isotropic creep models for the behavior of the grain material, various simple theoretical models were considered initially, such as the slip line approach of Brunner and Grant (1959), while shortly after, the phenomenon was studied more accurately by using numerical methods, first by Crossman and Ashby (1975) and culminating in Ghahremani's (1980) paper. The cited studies were all concerned with 2-D arrays of hexagonal grains. They have been complemented more recently by the 3-D works of Anderson and Rice (1985) and Dib and Rodin (1993).

In addition to creep rate enhancement, free sliding leads to an enhancement of the average normal stress transmitted by grain boundaries that are normal to the macroscopic maximum principal tensile stress direction. This has been discussed in a 2-D context by, e.g., Rice (1981) and for 3-D by Anderson and Rice (1985) and by Dib and Rodin (1993). As this so-called principal facet stress is an important driving force for the development of grain boundary cavitation, there is an obvious interest in adequate descriptions of this phenomena because of the implications for creep fracture (see, e.g., Nix *et al.*, 1989).

All 2-D studies mentioned above have used periodic arrangements of completely regular hexagonal grains. Similarly, the cited 3-D studies used regular truncated octahedrons as space-filling model grains. It is clear that grains in real materials vary in size

and shape throughout the polycrystal, but the effects of that on creep behavior have not been studied in the past, probably since the regular grains were considered to represent the 'average grain shape'. Rodin (1995) has very recently investigated the effect of variations in grain size and shape on the facet stresses, both in 2-D and in 3-D. On statistical grounds, he obtained expressions for the principal facet stress, which has to be interpreted as an average over the whole polycrystalline aggregate. Notably, the result for random 2-D aggregates is identical to that for an aggregate comprising regular hexagonal grains (Rice, 1981).

Recent findings by Van der Giessen and Tvergaard (1994b) have started to shed a different light on the effect of variations in microstructure. They developed a planar polycrystal model where a unit cell out of the aggregate contains a number of grains. In addition to grain boundary sliding, the model accounts for the nucleation and growth of cavities on the grain boundaries until coalescence leads to intergranular cracking. With this model they investigated the creep fracture process in polycrystalline aggregates with various microstructures, obtained by randomly changing the size and shapes of the grains, and found a remarkable sensitivity of the predicted time to failure on the microstructure when grain boundary sliding was assumed to be free. Although a statistically meaningful random variation was not feasible, their results indicated the possibility that the lifetime for an intuitively reasonable microstructure is a factor of five or so shorter than that for the reference microstructure with regular hexagonal grains. This rather extreme sensitivity has been attributed primarily to the free grain boundary sliding, as the influence of microstructure was found to be only a few percent when grain boundary sliding was not possible. Curving of the grain boundaries and small scale irregularities that increase the sliding resistance tend to reduce the sensitivity, as demonstrated by Van der Giessen and Tvergaard (1994c).

Van der Giessen and Tvergaard (1994b) related the sensitivity of predicted lifetimes under free sliding to the observation that the facet stresses scaled roughly inversely with the width of the facets. A further investigation (Onck and Van der Giessen, 1995) has subsequently revealed that the variations in microstructure also influenced the overall creep rate enhancement in the absence of cavitation. This is a phenomenon that has been anticipated in principle by Crossman and Ashby (1975) but the magnitude of the effect was found to be surprisingly large.

These latter findings in particular have motivated a more systematic study to trace back their origin and thus contribute to our insight in the effects of free sliding in irregular grain aggregates. In order to focus attention on the role of free grain sliding, the study reported on in this paper does not consider any cavitation damage. The objective of this paper is to reveal the fundamental features of how variations in grain geometry affect the response of the grains themselves, and therefore their collective behavior in an aggregate. To this end, the paper is structured as follows. We first discuss a number of general features of the overall behavior of aggregates of creeping grains (Section 2). Then, in Section 3, we confine further attention to planar arrays of freely sliding grains with random microstructures in terms of unit cell analyses. After illustrating some key features in terms of a small cell, single grain model (Section 4), we present the results of the numerical, multigrain cell model studies of aggregates with many different microstructures. In doing so, we focus on the overall creep rate enhancement (Section 5) as well as on the distribution of facet stresses in the aggregates (Section 6).

2. MACROSCOPIC BEHAVIOR

2.1. *General considerations*

We consider an aggregate of creeping grains, and ask for the relationship between the deformation behavior inside the grains (the 'microscopic' level) and the resulting overall response of the aggregate (the 'macroscopic' level) in the presence of free grain boundary sliding. To keep the presentation concise and in line with the existing literature on free grain boundary sliding, we assume that the creep behavior of the individual grains is incompressible and can be described by an isotropic, power-law creep relation. Denoting

all field quantities on the microscopic level by lowercase characters, this constitutive relation can be phrased in terms of the strain-rate potential

$$\phi = \frac{\sigma_0 \dot{\varepsilon}_0}{n+1}\left(\frac{\sigma_e}{\sigma_0}\right)^{n+1}, \tag{1}$$

as a function of the microscopic effective Mises stress

$$\sigma_e = (\tfrac{3}{2} s_{ij} s_{ij})^{1/2}, \tag{2}$$

with s_{ij} being the components of the stress deviator. Here, $\dot{\varepsilon}_0$ and σ_0 are reference strain-rate and stress quantities, and n is the creep exponent. The traceless creep strain-rate $\dot{\varepsilon}_{ij}$ inside the grains is obtained from (1) as

$$\dot{\varepsilon}_{ij} = \frac{\partial \phi}{\partial s_{ij}} = \dot{\varepsilon}_e \frac{3}{2}\frac{s_{ij}}{\sigma_e}, \tag{3}$$

with $\dot{\varepsilon}_e$ the effective creep rate defined by

$$\dot{\varepsilon}_e = (\tfrac{2}{3}\dot{\varepsilon}_{ij}\dot{\varepsilon}_{ij})^{1/2} = \dot{\varepsilon}_0\left(\frac{\sigma_e}{\sigma_0}\right)^n. \tag{4}$$

We now consider an aggregate of such grains and ask for the overall (macroscopic) response to a macroscopic state of stress with deviatoric components S_{ij}. From dimensional considerations it follows that the macroscopic creep potential Φ must be of the form

$$\Phi = (\sigma_0 \dot{\varepsilon}_0) F\left(\frac{S_{ij}}{\sigma_0}, n, \mathscr{S}\right), \tag{5}$$

where $\mathscr{S}$ represents the microstructure, i.e., the geometrical information of the aggregate and the constituting grains. With the grains being able to freely slide against each other, the overall response depends on $\mathscr{S}$ through the spatial distribution of the sliding grain boundaries relative to the macroscopic stress directions. As sliding itself is a volume preserving deformation mode, the overall creep rate $\dot{E}_{ij}$ is traceless, provided that the grain arrangement is space-filling (or area-filling in 2-D).

In general, the overall behavior cannot be expected to be isotropic and will be determined by the functional dependence of Φ on S_{ij} through $\mathscr{S}$. In the special case that the aggregate is isotropic, the stress dependence can be captured by the overall (macroscopic) Mises stress, and the macroscopic creep potential for *isotropic aggregates* of sliding grains can be written as

$$\Phi = \frac{\sigma_0 \dot{\varepsilon}_0}{f^*(n+1)}\left(f^* \frac{\Sigma_e}{\sigma_0}\right)^{n+1}, \quad \Sigma_e = (\tfrac{3}{2} S_{ij} S_{ij})^{1/2}. \tag{6}$$

By differentiation with respect to S_{ij} it follows that

$$\dot{E}_{ij} = \dot{E}_e \frac{3}{2}\frac{S_{ij}}{\Sigma_e}, \quad \dot{E}_e = \dot{\varepsilon}_0\left(f^* \frac{\Sigma_e}{\sigma_0}\right)^n. \tag{7}$$

The parameter f^* in (6) and particularly in the overall effective creep rate $\dot{E}_e$ in (7) has been introduced by Crossman and Ashby (1975) as the *stress enhancement factor*. In the absence of sliding, $f^* = 1$ and the macroscopic and microscopic response are equivalent. Comparing

the expression for $\dot{E}_e$ with that for the microscopic counterpart $\dot{\varepsilon}_e$ in (4) leads to the interpretation that free sliding enhances the driving force Σ_e for macroscopic creep by a factor f^*. Looking at (6) it appears that one can alternatively interpret f^* to reduce the creep reference stress σ_0 by a factor $1/f^*$. In the case of planar polycrystals, macroscopic isotropy is achieved for a doubly-periodic packing of perfect regular hexagonal grains, for which the six-fold symmetry implies isotropy. Making use of that, Ghahremani (1980) has accurately computed the values of f^* ($f^* > 1$) for a range of creep exponents n.

When an aggregate consists of irregular hexagonal grains in 2-D, macroscopic isotropy is lost. In 3-D, overall isotropy is not even obtained by the 3-D counter-part of hexagons, i.e., truncated octahedra as considered by Anderson and Rice (1985) and Dib and Rodin (1993). For each particular aggregate contained in the representative volume element, the macroscopic creep potential Φ in (5) can formally be obtained from (1) by homogenization methods (see Hill, 1967). Unfortunately, this appears to be unfeasible for the present highly nonlinear problem (perhaps, the nonlinear bounding techniques developed, e.g., by Ponte Castañada (1991) may be used, but the accuracy would remain to be established). Therefore, for the matter of illustration and for future reference, we shall assume that there is a *class of anisotropic aggregates* for which the stress dependence of the function F in (5) can be written in terms of a scalar-valued equivalent stress

$$\bar{\Sigma} = (\tfrac{3}{2} S_{ij} M_{ijkl} S_{kl})^{1/2} \tag{8}$$

such that Φ can be written in the form

$$\Phi = \frac{\sigma_0 \dot{\varepsilon}_0}{f^*(n+1)} \left(f^* \frac{\bar{\Sigma}}{\sigma_0} \right)^{n+1}, \tag{9}$$

similar to (6). The coefficients $M_{ijkl} = M_{klij} = M_{lkij} = M_{lkji}$ account for the macroscopic anisotropy, and are necessarily positive definite. Note further that due to the deviatoric nature of the S_{ij}, spherical symmetric parts in both the ij and kl indices of M_{ijkl} do not contribute to $\bar{\Sigma}$, so that there are only 15 independent coefficients. In the case of isotropy, they reduce to the fourth-order unit tensor $I_{ijkl} = \frac{1}{2}(\delta_{ik}\delta_{jl} + \delta_{il}\delta_{jk})$, so that $\bar{\Sigma} = \Sigma_e$ (cf. (6)). Therefore, M_{ijkl} can be regarded as a correction m_{ijkl} on this, i.e.,

$$M_{ijkl} = I_{ijkl} + m_{ijkl}. \tag{10}$$

The potential (9) now leads to

$$\dot{E}_{ij} = \dot{\bar{E}} \frac{3}{2} M_{ijkl} \frac{S_{kl}}{\bar{\Sigma}}, \tag{11}$$

with $\dot{\bar{E}}$ being defined by

$$\dot{\bar{E}} = \left(\frac{2}{3} \dot{E}_{ij} M^{-1}_{ijkl} \dot{E}_{kl} \right)^{1/2} = \dot{\varepsilon}_0 \left(f^* \frac{\bar{\Sigma}}{\sigma_0} \right)^n. \tag{12}$$

Compared with the overall creep rate components in the absence of grain boundary sliding, the creep rates $\dot{E}_{ij}$ according to (11) are multiplied by factors $(f^*)^n M_{ijkl}$; in other words, each creep component has its own stress enhancement factor. Taking into consideration the number of independent coefficients in M_{ijkl} or m_{ijkl}, this means that there are in general 15 different stress enhancement factors.

The coefficients M_{ijkl} can be regarded as the components of a fourth-order tensor $\mathbf{M}$ on the same basis as used for the macroscopic stress components S_{ij}. This tensor depends on the microstructure of the aggregate defined by the size and shape of the grains. Phrased differently, $\mathbf{M}$ depends on the location, orientation and shape of the grain facets and their

connectivity. In this sense, the **M** are akin to the fourth-order crack density tensors of Kachanov (1992) to describe the overall effect of a distribution of cracks in an elastic medium. But, because of the different physical interpretations, one cannot expect that application of the form of such crack density tensors is successful in incorporating the influence of microstructure on the overall creep response with free grain boundary sliding.

2.2. *Planar polycrystals*

To fix ideas and for further use in the next sections, let us consider a planar polycrystal that is constructed by means of a space-filling packing of arbitrarily shaped polygonal grains as illustrated in Fig. 1. All grains are prismatic in the x_3-direction perpendicular to the plane of interest, and have the same thickness. With proper boundary conditions, all fields are homogeneous in the x_3-direction, so that we arrive at a planar polycrystal. To be more specific, we imagine the aggregate to be subjected to boundary conditions, especially on the faces normal to x_3, such that plane strain conditions apply on the microscopic scale, i.e., $\dot{\varepsilon}_{i3} = 0$ everywhere in the grains. Indeed, this conforms with the specific problem that will be formulated in Section 3. Due to the microscopic isotropy of the grain material, (3) yields $s_{13} \equiv 0$ so that $S_{i3} = 0$. Thus, the planar creep rates $\dot{E}_{\alpha\beta}$ are given by

$$\dot{E}_{\alpha\beta} = \dot{\bar{E}} \frac{3}{2} M_{\alpha\beta\kappa\lambda} \frac{S_{\kappa\lambda}}{\bar{\Sigma}}. \tag{13}$$

As a consequence of the resulting in-plane incompressibility, $\dot{E}_{\alpha\alpha} = 0$, there are only three independent coefficients $M_{\alpha\beta\kappa\lambda}$ in (13). This can be made explicit by augmenting the condition $M_{\alpha\alpha\kappa\lambda} S_{\kappa\lambda} = 0$ with the side condition $\delta_{\kappa\lambda} S_{\kappa\lambda} = 0$, yielding

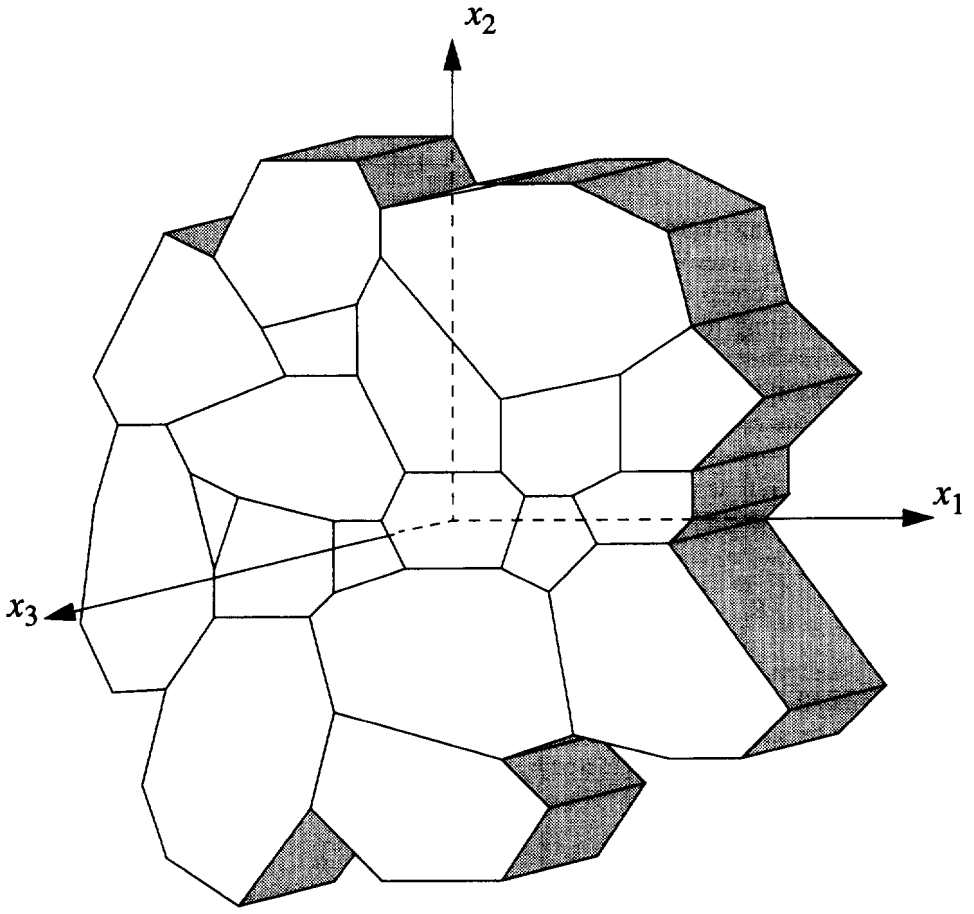

Fig. 1. Polycrystalline aggregate of prismatic grains: a planar polycrystal model.

$$M_{1111} = M_{2222}, \quad M_{1111} + M_{1122} = 1, \quad M_{1112} + M_{2212} = 0. \tag{14}$$

Furthermore, the requirement that the M_{ijkl} be positive definite can in this case readily be specified as

$$M_{1111} > 1/2, \quad M_{1212} > 0, \quad (M_{1112})^2 < M_{1212}(M_{1111} - 1/2). \tag{15}$$

Evidently, for an anisotropic polycrystal as illustrated in Fig. 1 it is not sufficient to consider a single stress enhancement factor. That is, the definition of a stress enhancement factor must be associated with a particular state of stress relative to the microstructure of the material. An obvious procedure is to define stress enhancement factors under uniaxial states of stress with different stress directions with respect to the microstructure (in a 3-D context, this has been done by Dib and Rodin, 1993). For the planar polycrystal at hand here, one may, for example, consider (plane strain) *uniaxial tension along the x_1-direction* indicated in Fig. 1 at a stress level Σ. In that case, $\Sigma_{11} = \Sigma$, $\Sigma_{22} = 0$, so that $S_{11} = -S_{22} = \frac{1}{2}\Sigma$, $\Sigma_e = \frac{1}{2}\sqrt{3}\Sigma$ and $\bar{\Sigma} = \Sigma_e\sqrt{2M_{1111} - 1}$. It then follows from (13) that

$$\dot{E}_{11} = \frac{3}{4}\dot{\varepsilon}_0\left(\frac{\Sigma_e}{\sigma_0}\right)^n (f_{11})^n \frac{\Sigma}{\Sigma_e}, \tag{16}$$

where we have substituted

$$f_{11} = f^*(2M_{1111} - 1)^{(n+1)/2n}. \tag{17}$$

The creep rate according to (16) now contains the factor $(f_{11})^n$ over the expression in the absence of sliding (obtained by inserting the macroscopic stress Σ_{ij} into (1)–(4)). Thus, f_{11} is naturally termed the enhancement factor for uniaxial creep in the x_1-direction. In a similar manner, one can consider *uniaxial creep in the x_2-direction*, for which one then finds an expression for $\dot{E}_{22}$ which is fully similar to the right-hand side in (16), but with f_{11} being replaced with f_{22} defined by

$$f_{22} = f^*(2M_{2222} - 1)^{(n+1)/2n}. \tag{18}$$

We note that according to (14), we have $f_{11} = f_{22}$. Thus, for planar polycrystalline aggregates that are governed by macroscopic creep potentials of the form (9), the stress enhancement factors for uniaxial creep in two mutually orthogonal directions are identical. From the considerations relating to (13) and (14), it is clear that this is a simple consequence of planar incompressibility. Finally, in a similar fashion one can relate the stress enhancement factor f_{12} in shear in the x_1–x_2-plane to the anisotropy coefficient M_{1212}.

In general, the creep response of the planar polycrystal with free sliding will not be orthotropic. This implies for instance that if it is subjected to uniaxial tension in the x_1-direction with $\Sigma_{12} = 0$ as above, it will respond with a non-zero shear creep rate, which according to (13) is given by

$$\dot{E}_{12} = \frac{3}{4}\dot{\varepsilon}_0\left(\frac{\Sigma_e}{\sigma_0}\right)^n (f^*)^n (2M_{1111} - 1)^{(n-1)/2} 2M_{1112}\frac{\Sigma}{\Sigma_e}. \tag{19}$$

Thus, the nonorthotropy is governed by the parameter M_{1112}. If, instead, $\dot{E}_{12}$ is imposed to be zero during tension, a non-zero shear stress Σ_{12} is necessary to enable this. In that case, however, the stress enhancement factor f_{11} is no longer given by the simple expression (17).

3. PROBLEM FORMULATION AND METHOD OF SOLUTION

To quantify the foregoing considerations for planar polycrystalline aggregates, we adopt the multi-grain unit cell model of a 2-D polycrystal used earlier for creep rupture

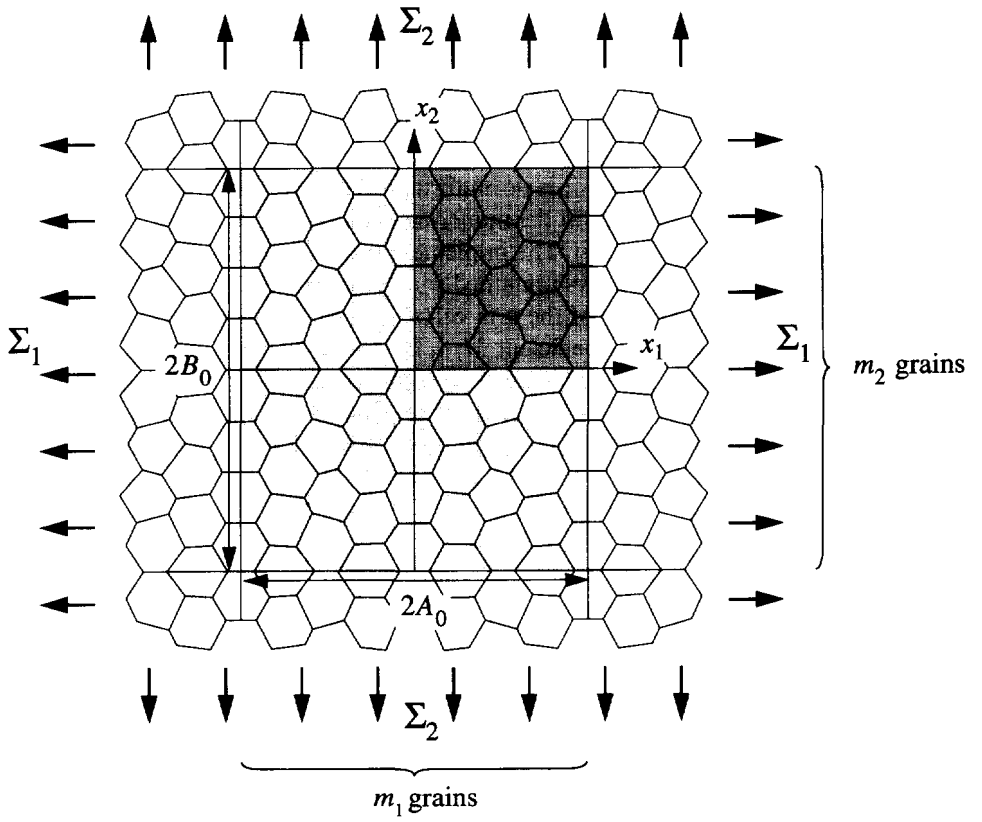

Fig. 2. The polycrystal unit cell model comprising $m_1 \times m_2$ grains. Only the dark shaded region is analyzed.

studies by Van der Giessen and Tvergaard (1994a–c). The formulation of that model being described in the cited references, we give only a brief recapitulation here.

The model material is built up as an array of arbitrarily shaped, but hexagonal grains. The microstructure of the material, being defined by the collection of grain sizes and shapes, is assumed to reflect a certain periodicity that allows for the identification of a unit cell, as shown in Fig. 2. Let $2A_0$ and $2B_0$ be the undeformed dimensions of the unit cell in the x_1 and x_2 directions, respectively, and let the cell contain $m_1 \times m_2$ grains. The cell shown in Fig. 2 is characterized by $(m_1, m_2) = (8, 8)$. Further, the unit cell itself is assumed to exhibit reflective symmetries with respect to its four sides, so that only a quarter of the unit cell needs to be analyzed.

Under plane strain conditions in the x_3-direction, the material is subjected to constant in-plane principal stresses $\Sigma_{11} = \Sigma_1$ and $\Sigma_{22} = \Sigma_2$ (see Fig. 2). By virtue of its symmetries, the quarter cell boundaries are required to remain straight and shear stress free. With A and B denoting the deformed dimensions of the quarter cell, the macroscopic creep rates and macroscopic stress are computed as

$$\dot{E}_{11} = \dot{A}/A, \quad \dot{E}_{22} = \dot{B}/B \tag{20}$$

$$\Sigma_1 = \frac{1}{B}\int_0^B \sigma_{11}(A, x_2)\,\mathrm{d}x_2, \quad \Sigma_2 = \frac{1}{A}\int_0^A \sigma_{22}(x_1, B)\,\mathrm{d}x_1. \tag{21}$$

The material inside the grains is taken to be homogeneous and to deform primarily by power-law creep as described by (1)–(4). For computational convenience, isotropic elasticity of the grain material is accounted for, governed by the Young's modulus E and Poisson's ratio ν. All results to be presented here pertain to states in which any initial elastic effects have relaxed so that a steady-state creep situation has been reached and the elastic properties are irrelevant.

The grains in the polycrystal are discretized using quadrilateral finite elements, each built up of four constant strain triangles which are arranged in a 'crossed triangle' configuration. The finite element mesh is generated by mapping each grain to a reference, regular hexagonal grain, then creating the mesh and finally mapping back in an affine manner to the irregular grain shape. Free grain boundary sliding is implemented through special interface elements, which support normal stresses in a very stiff manner, but do not transmit any shear stress. For details of the numerical method, the reader is referred to Van der Giessen and Tvergaard (1994a, b). The implementation accounts for finite strains even though in this study the strains always remained smaller than 2%.

Due to the assumed symmetry of the unit cell shown in Fig. 2, the material is macroscopically orthotropic, so that the coefficient M_{1112} in (13) and (19) vanishes. Therefore, in this analysis only a single stress enhancement factor needs to be considered, namely $f = f_{11} = f_{22}$. For the case of, for instance, uniaxial tension in the x_2-direction ($\Sigma_1 = 0$), the value of the stress enhancement factor f is obtained from the computed creep rate $\dot{E}_{22}$ through

$$f = \left(\frac{\dot{E}_{22}}{\dot{\varepsilon}_{22}}\right)^{1/n}, \tag{22}$$

where $\dot{\varepsilon}_{22}$ is the strain rate in the absence of sliding, which is equal to the microscopic strain-rate obtained by substituting the applied macroscopic stress Σ_2 into (3).

4. SINGLE GRAIN MODEL AND ESTIMATES

As a first step in quantifying the effect of variations in microstructure on creep rate enhancement and facet stresses, we consider a polycrystal that exhibits a high level of periodicity, so that we confine attention to a small unit cell characterized by $(m_1, m_2) = (2, 1)$. Figure 3 shows a quarter of the (2, 1) unit cell. This problem refers to an aggregate consisting of identical grains, the geometry of which can be described in terms of four dimensionless variables, B_0/A_0, R_0/A_0, C_0/A_0 and φ, of which only two are independent (see Fig. 3). If we choose to use R_0/A_0 and φ as independent parameters, the perfectly regular hexagonal microstructure corresponds to $R_0/A_0 = 1/3$ and $\varphi = 60°$.

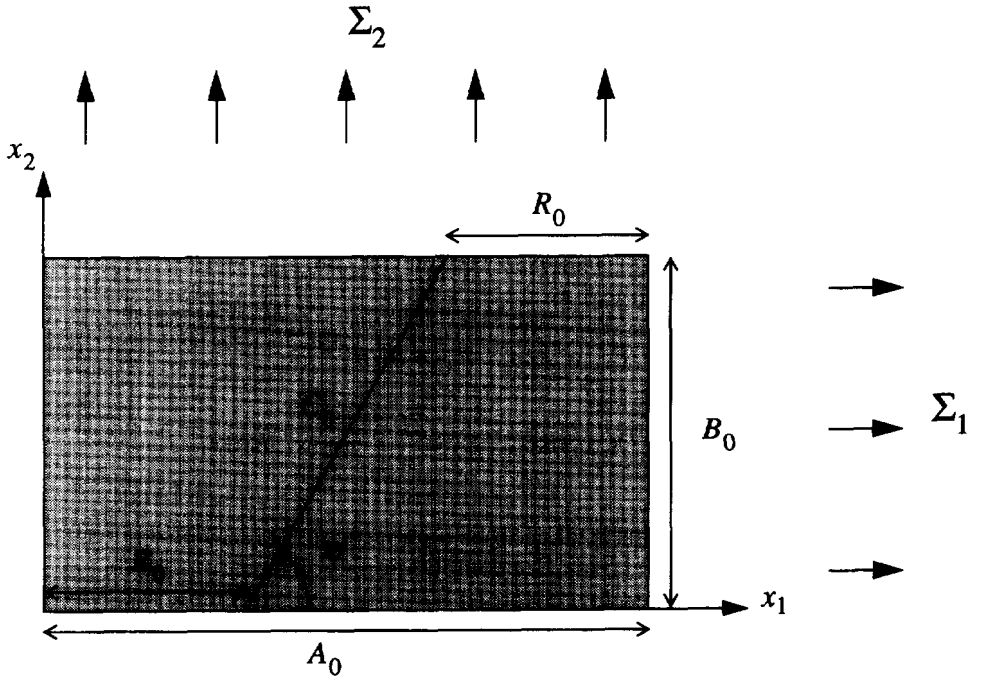

Fig. 3. The single grain model, corresponding to a quarter of the (2, 1) unit cell.

The absence of shear stresses at the grain boundaries renders this aggregate to be statically determined. For regular hexagonal grains, this was used by Cocks and Ashby (1982) to calculate the so-called facet stresses, i.e., the average normal stresses at the grain boundary facets, for a general 2-D stress state. This exercise can be easily repeated for the single grain model in Fig. 3 with grains that are not regular hexagons, yielding

$$\sigma_n^{tr} = \Sigma_1 + \frac{1}{2}\frac{A_0}{R_0}(\Sigma_2 - \Sigma_1), \tag{23}$$

$$\sigma_n^{in} = \Sigma_1, \tag{24}$$

where σ_n^{tr} and σ_n^{in} denote the facet stress on the transverse (R_0) and inclined (C_0) facets, respectively. It is clear that the amplification of the facet stress σ_n^{tr} over the applied stress Σ_2 due to grain boundary sliding is affected only by R_0/A_0 and is independent of the sliding facet orientation φ. Note that for a regular hexagonal microstructure under uniaxial tension in the x_2-direction ($\Sigma_1 = 0$), we recover $\sigma_n^{tr} = 1.5\Sigma_2$, as mentioned by Rice (1981).

In the forthcoming section, numerical results shall be presented for the creep rate enhancement due to sliding in the single grain model for various grain shapes. In addition to these detailed full field results, we shall also attempt two simple analytical estimates. These estimates are based on two of the numerous simple models that have been proposed in the literature as estimates for the influence of grain boundary sliding on the overall strain rate in regular hexagonal polycrystals, but now extended to the more general microstructure of Fig. 3.

- *Slip line model*
  In the limit of $n \to \infty$ the grain material behaves (elastic-) perfectly plastic. Neglecting elasticity, the contribution of freely sliding grain boundaries to the overall strain-rate can be deduced from slip line theory, as proposed by Brunner and Grant (1959). For simple shear parallel to the x_1-direction there is just one slip line, connecting the grain boundaries in the shear direction. Since the ratio of slip line to grain boundary facet length is 3/2, the stress needed to flow the material is reduced by a factor 2/3. This can be related to a stress enhancement factor for shear of 1.5. For uniaxial tension in the x_2-direction Brunner and Grant (1959) present the slip lines in a grain as observed from experiments. Chen and Argon (1979) assume the slip lines to be identical for uniaxial tension in the x_1-direction and arrive at a stress enhancement factor for tension to be $1.5 \sin 120° = 1.3$. Although this slip line approach does not result in a unique stress enhancement factor, as is required for regular hexagonal grains (cf. Sec. 2), it does indicate that the interaction of co-linear grain boundary facets is of importance in determining the stress enhancement. In spite of the fact that the interaction decreases with decreasing stress exponent n, as shown by Crossman and Ashby (1975), we adopt the idea to obtain an estimate for the single grain model (Fig. 3). The result reads

$$f^{sl} = \left(1 + \frac{C_0}{D_0}\right)\sin 2\varphi, \tag{25}$$

where $D_0 = 2\sqrt{R_0^2 + B_0^2}$ is the length of the diagonal of the grain.

- *Shear crack model*
  The relative sliding velocity, $\dot{u}$, on a grain boundary facet is zero at the triple points and reaches a maximum at the center. According to Brunner and Grant (1959), the contribution of a single sliding grain boundary to the total elongation is calculated from the average sliding displacement across the facet. This method was used by Riedel (1984) to approximate the stress enhancement factor in a regular hexagonal microstructure under uniaxial tension. The average sliding displacement rate was

estimated on the basis of that for an isolated facet in a linear material. Finally, the expression for the stress enhancement factor followed from the assumption that the total strain rate in a sliding material simply is the sum of the uniform strain rate in a non-sliding material and the contribution due to free sliding. This analysis is repeated for the single grain model in the Appendix and yields

$$f^{sc} = \left(1 + \frac{\pi}{8}\sqrt{n}\frac{C_0^2}{A_0 B_0}\sin^2 2\varphi\right)^{1/n}. \tag{26}$$

5. CREEP ENHANCEMENT

In this section we numerically investigate the influence of geometrical variations on the stress enhancement factor f for creep both in terms of the single grain model (see Section 5.1) and for random variations in a large unit cell (see Section 5.2). All computations have been carried out for uniaxial tension at constant Σ_2 ($\Sigma_1 = 0$) corresponding to an applied effective stress of $\Sigma_e = \frac{1}{2}\sqrt{3}\Sigma_2$, and for different values of the creep exponent n. All results to be reported pertain to states of steady-state creep which are attained after any elastic effects have relaxed (the elastic properties were chosen such that $v = 1/3$ and $\Sigma_e/E = 0.5 \times 10^{-3}$ which ensures that elastic strains are negligible).

5.1. *Single grain model*

Figure 4 shows the finite element mesh for the single grain problem with regular hexagonal microstructure ($R_0/A_0 = 1/3$ and $\varphi = 60°$) used in our computations. Each quadrilateral consists of four 'crossed triangles', while a refinement is used along the grain boundaries. As we shall see later, because of the relaxation of shear stress at the grain boundaries, the stress state in the grains becomes highly nonuniform and even singular very close to the triple points (Lau and Argon, 1977). Hence, the numerical results are sensitive to the choice of mesh (also see Ghahremani, 1980). The discretization shown in Fig. 4 results in a stress enhancement factor $f = 1.198$ for $n = 5$, which coincides with Ghahremani's (1980) result. An increase of the number of elements by a factor 2 yields an increase in f of 0.6%, showing a rapid convergence for this discretization and microstructure. Hence, the meshes for other values of R_0/A_0 and φ were chosen to have the same number of elements, and are generated by an affine mapping onto the regular geometry (cf. Section 3).

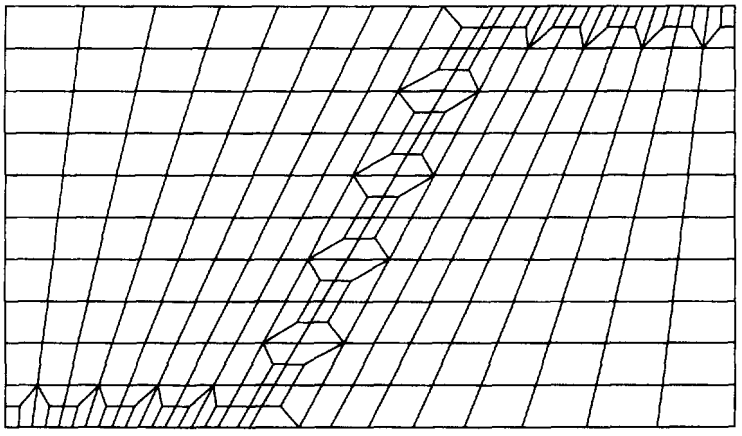

Fig. 4. Finite element mesh for a quarter of the (2, 1) unit cell, for a regular hexagonal microstructure. Each quadrilateral consists of four 'crossed triangles'.

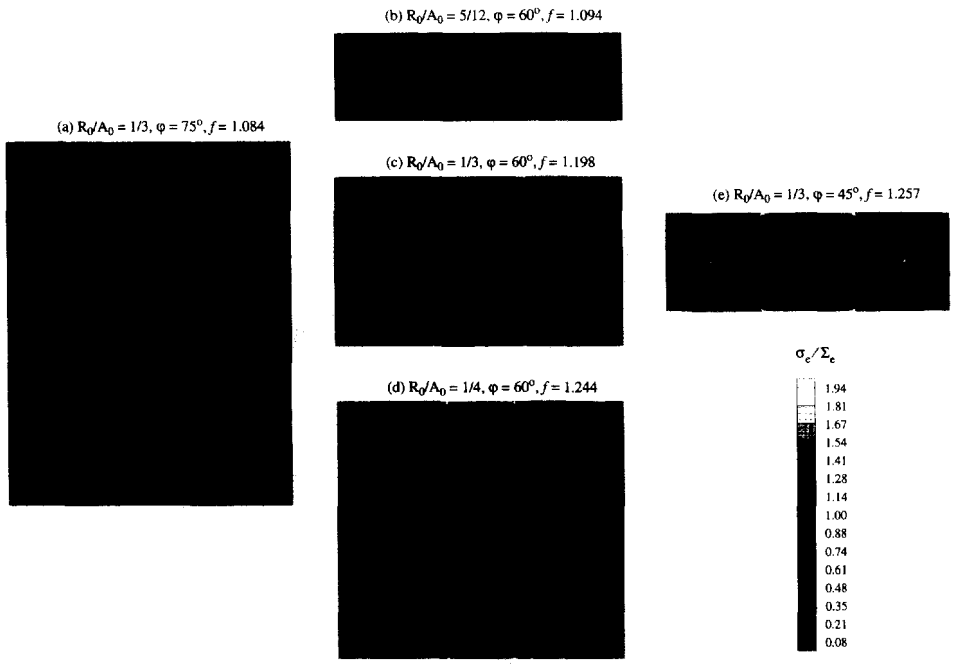

Fig. 5. Contour plots of normalized effective stress for five realizations of the single grain model, showing the influence of the variables R_0/A_0 and φ on the stress distribution and stress enhancement factor f.

Figure 5 shows the distributions of the (steady state) effective stress, normalized by the applied effective stress, σ_e/Σ_e, for five realizations of the model problem with $n = 5$. For each realization, also the computed stress enhancement factor f is shown. The plots are generated by making use of the reflective symmetries of the unit cell, in order to get a clear picture of the stress distribution in the grains. Note that A_0 is kept fixed in all cases considered. The influence of φ is shown in the horizontal direction by Figs 5(a), 5(c) and 5(e). It is clear that a decrease in φ results in an increase in the stress enhancement factor. This can be attributed to a 'wedge' effect, causing the stress distribution to be more nonuniform, resulting in a higher average effective stress in the grains and thus in an enhancement of the macroscopic creep rate. Increasing the angle further to 90°, would result in a uniform stress distribution corresponding to $f = 1$. The influence of R_0/A_0 is shown in the vertical direction by Figs 5(b), 5(c) and 5(d). Decreasing the width of the transverse facets is seen to increase the stress enhancement factor. This can be related to the reduction in load carrying area fraction, which is also responsible for the increase in transverse facet stress, according to (23).

From the above considerations it is clear how the stress enhancement factor in the single grain model depends both on R_0/A_0 and φ in a qualitative manner. We will now investigate whether the simple models, described in the previous section, capture these dependencies quantitatively. In addition to the five realizations shown in Fig. 5, we have analyzed five extra cases, in which both R_0/A_0 and φ are varied simultaneously. Figure 6(a) compares the approximate expression based on the slip line model f^{sl}, according to (25), with numerical results for f, for a creep exponent $n = 5$. As expected, the absolute values of f are predicted poorly, since the model is based on slip line theory ($n \to \infty$). The influence of the grain geometry, however, is picked up qualitatively, although it is overestimated somewhat. The same calculations are carried out for $n = 10$ in Fig. 6(b). This larger value of n yields somewhat higher values of f than for $n = 5$ (cf. Ghahremani, 1980), but the correlation between f^{sl} and f does not seem to be significantly improved.

Figure 6(c) shows the same numerical results as Fig. 6(a), but now confronted against the expression for the shear crack model, f^{sc}. Again the influence of the geometry is captured well, although underestimated slightly. Figure 6(d) denotes the results of the shear crack model for $n = 1$, showing an almost perfect correlation. The good correlation between f^{sc}

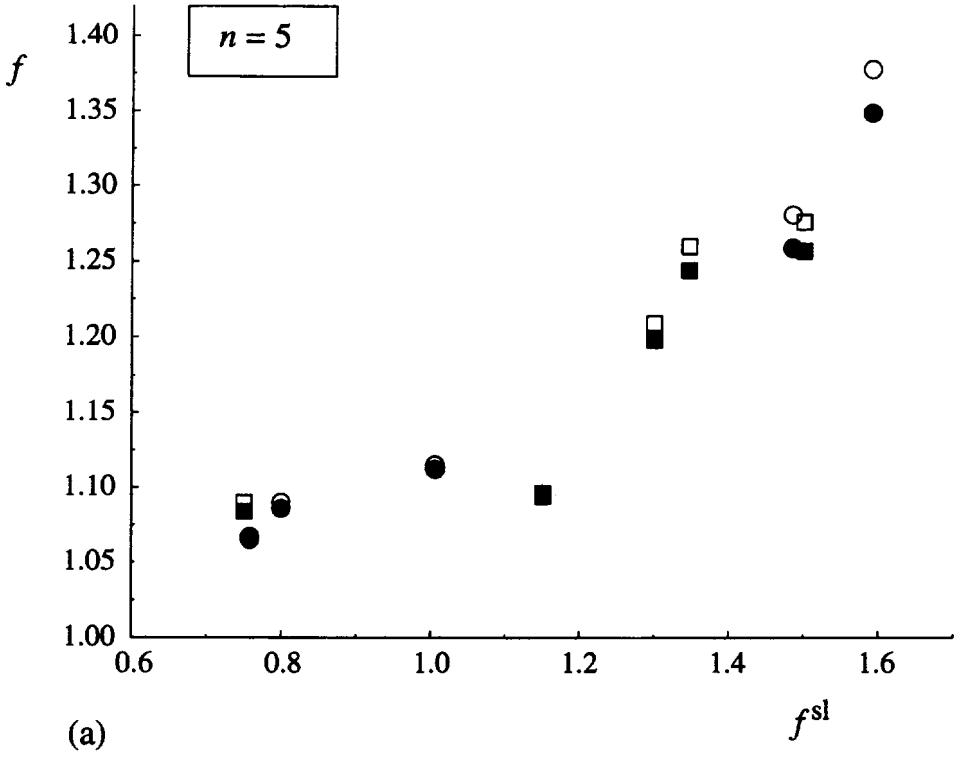

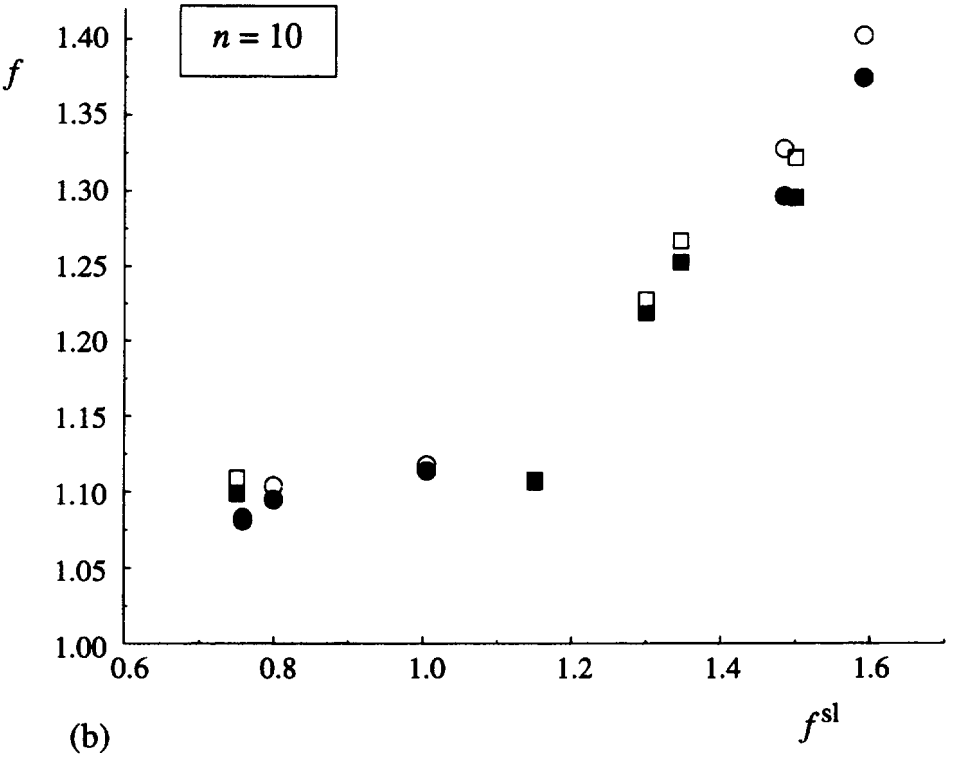

Fig. 6. Verification of the simple models by comparison of the approximate expressions, f^{sl} and f^{sc}, for the stress enhancement factor with numerical results, f. The squares correspond to the realizations of Fig. 5, the circles are additional realizations for the problem of Fig. 3. Open symbols denote results obtained with an improved mesh. (a) Slip line model, $n = 5$; (b) slip line model, $n = 10$; (c) shear crack model, $n = 5$; (d) shear crack model, $n = 1$.

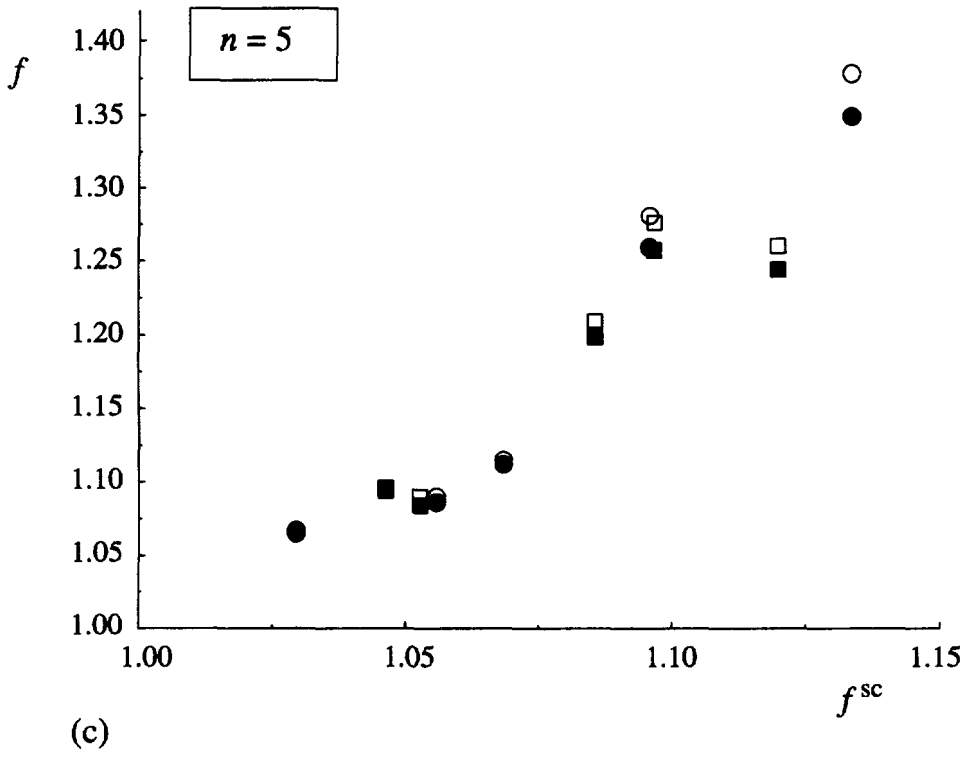

(c)

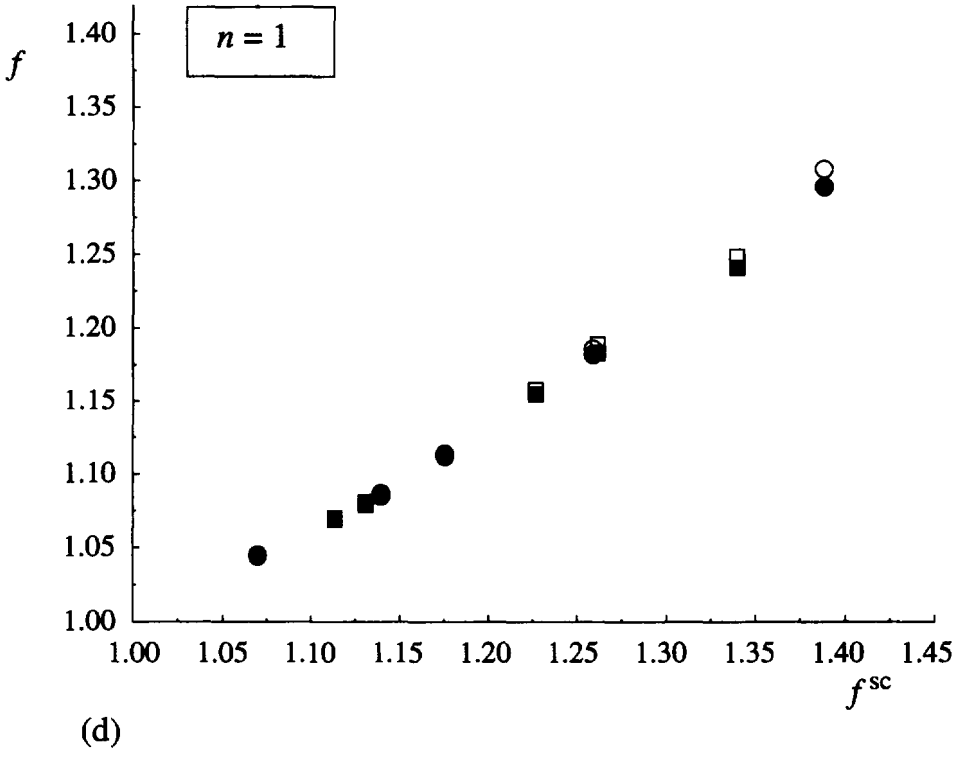

(d)

Fig. 6. *Continued.*

and f for $n = 1$ can be partly attributed to the fact that the shear crack model is based on a linearization of the material law, which would yield exact results for the average relative sliding velocity along the grain boundaries when interactions between them can be neglected. Moreover, the interaction between sliding grain boundaries indeed decreases with decreasing values of n (Crossman and Ashby, 1975). For increasing n, the interaction between grain boundaries is responsible for the deteriorating performance of f^{sc} as an estimate for f. Further, Figs 6(c) and 6(d) show that the f^{sc} exhibits an incorrect dependence on the creep exponent n.

To investigate the influence of the discretization for irregular microstructures, we have repeated the calculations using an improved mesh with twice as many elements. Furthermore, for realizations that lead to distorted elements, caused by the mentioned mapping strategy, the aspect ratio of the elements was restored to unity. The improved mesh computations are denoted by open symbols in Fig. 6 and show that the stress enhancement factor is in all cases slightly underestimated, especially for larger n.

5.2. *Random variations*

Although the single grain model problem considered in the previous section has highlighted some key geometrical factors in the microstructure that can have a significant influence on the macroscopic creep rate enhancement, it still represents a highly periodic, rather regular microstructure. All grains have the same shape and they are always oriented along the principal axes. To introduce more variation into the analysis, we now consider larger unit cells with $(m_1, m_2) = (8, 8)$, as shown in Fig. 2. Random microstructures are generated by imposing random variations on the regular hexagonal microstructure. These variations are limited to such an extent that the grains remain hexagonal. Three different kinds of variations are used:

1. *Voronoi nuclei variations.* The regular hexagonal structure can be seen as the Voronoi tessellation of a uniform distribution of nuclei over the plane, i.e., the distance between all nuclei is the same. Geometrical variations in the Voronoi tessellation are introduced by giving the positions of these nuclei a random offset.
2. *Triple point variations.* Variations are introduced by giving the triple grain junctions a random offset.
3. *Grain growth rate variations.* The nuclei of the regular hexagonal structure are given a random offset, like under 1. Furthermore, to each grain nucleus a radial growth rate is attributed which is randomly picked from a Gaussian distribution. Finally the position of the triple grain junctions are constructed in an approximate manner from the collision of expanding neighboring grain fronts.

It is emphasized that each of these three methods are purely 'mathematical' exercises; they should not be identified with actual physical mechanisms. Figure 7 shows examples of the

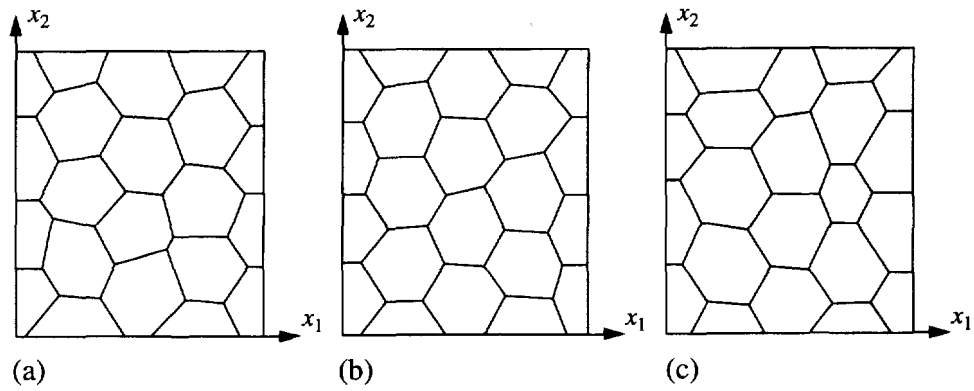

Fig. 7. Random variations in the microstructural geometry inside a quarter of the (8, 8) unit cell. (a) Type 1: variation in Voronoi nuclei location, (b) Type 2: variation in triple point position, (c) Type 3: variation in radial grain growth rate.

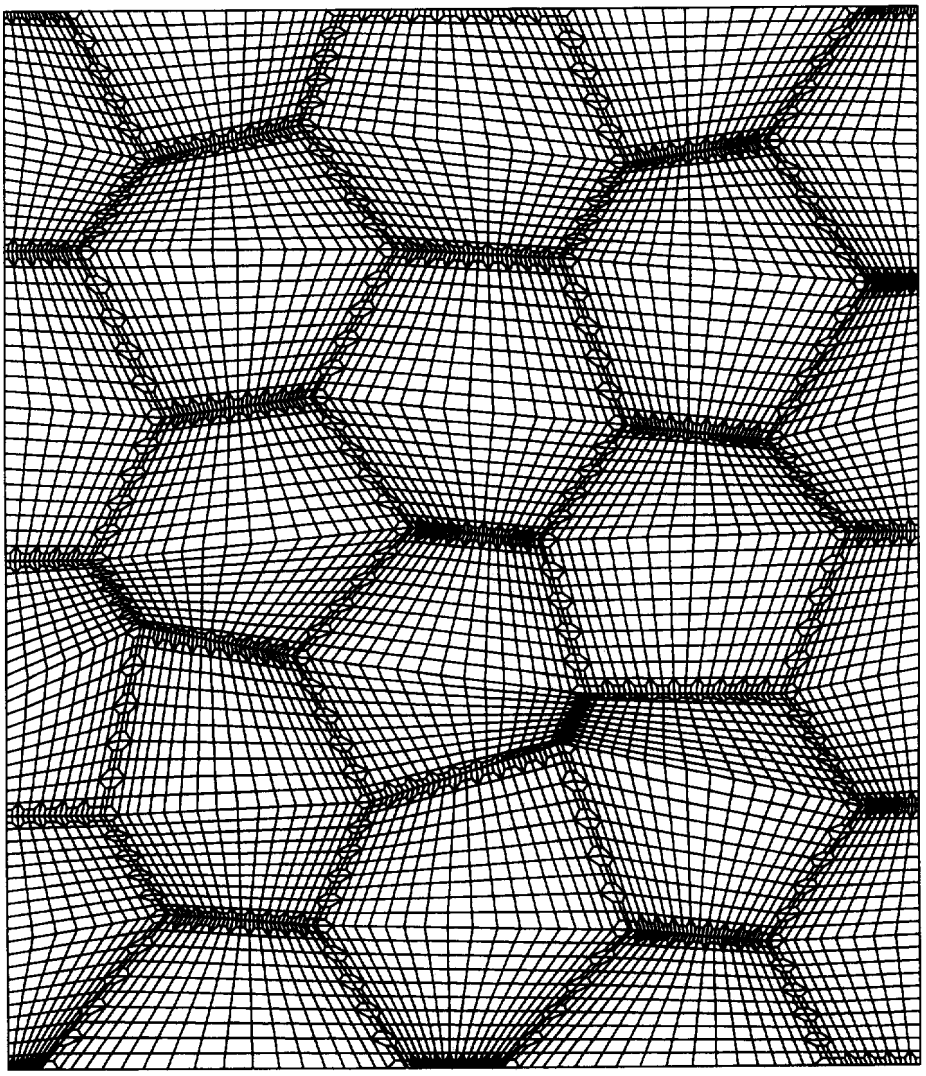

Fig. 8. Finite element mesh for a random realization of a quarter of the (8, 8) unit cell, corresponding to Fig. 7(a).

three different types of microstructures. Three different methods of generating microstructures have been used to avoid any bias in the results on the basis of the precise method of generation. Indeed, it will be seen later that although the microstructure in Fig. 7(b) appears to be less random than in Fig. 7(a), its effect on the macroscopic behavior is more pronounced. Microstructures of type 2 and 3 have been used previously by Van der Giessen and Tvergaard (1994b and 1994c, respectively) in their study of the influence of random variations on creep rupture. Note that in generating the microstructures, special care is taken of the facets touching the boundary of the quarter unit cell in order to preserve the symmetry properties.

We have generated 27, 13 and 12 microstructures of type 1, 2 and 3, respectively. The same material parameters are used as for the single grain model in Section 5.1 and the same uniaxial tension conditions are studied. The finite element discretization is again based on an affine mapping strategy. The reference mesh corresponds to Fig. 4, while an example of a typical mesh, corresponding to the microstructure of Fig. 7(a), is shown in Fig. 8.

The stress enhancement factors for all these microstructures have been computed for $n = 5$. The most important observation of the results is that the stress enhancement factors all exceed the value of $f = 1.198$ for the regular microstructure. Thus, for the large unit cell containing many grains, any random variation on the regular hexagonal structure leads to an increase in f, despite the fact that grain shapes exist that render a reduction of stress

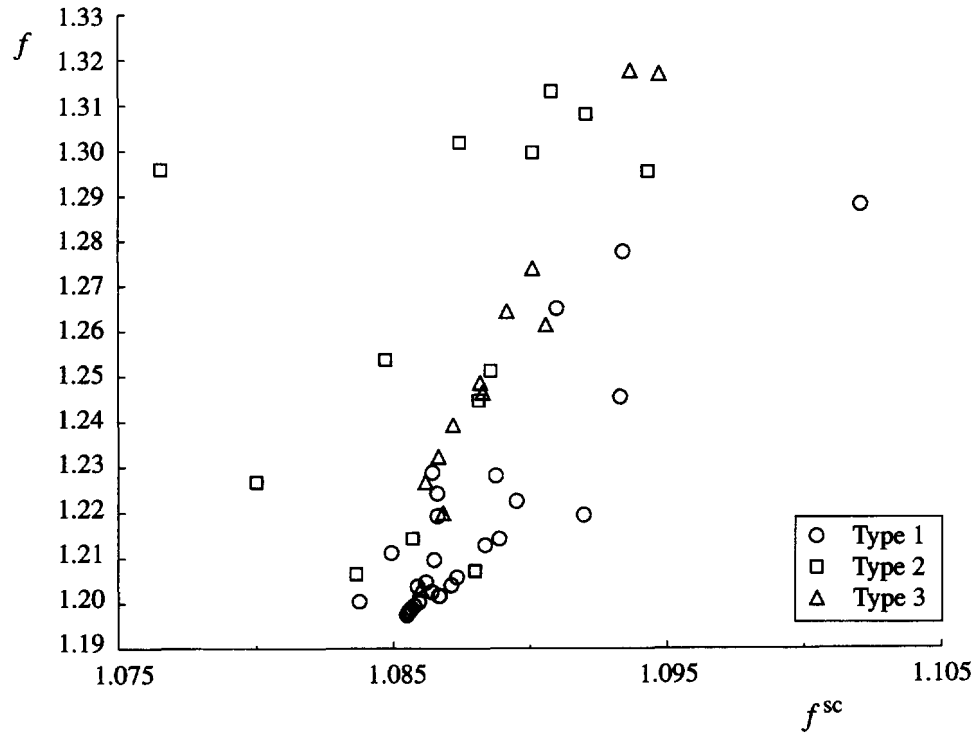

Fig. 9. Numerical values of the stress enhancement factor f for $n = 5$ for a number of random realizations of the (8, 8) unit cell, plotted vs the shear crack estimate f^{sc}, according to (27). The different symbols indicate the three types of microstructures generated by different methods, as discussed in the text.

enhancement factor in the single grain microstructure of Section 5.1. The largest value of f we have found for the random (8, 8) unit cell is around 1.32; this amounts to a 60% higher creep rate than according to the reference value of $f = 1.198$.

Just as for the single grain model discussed before, we wish to correlate the numerical results to analytical estimates. In Section 4 an estimate for the stress enhancement factor, f^{sc}, was derived for the single grain problem, based on the shear crack model. The expression (26) can be generalized to a random polycrystal, resulting in

$$f^{sc} = \left(1 + \frac{\pi}{2}\sqrt{n}\sum_j \frac{R^{(j)^2}}{A_0 B_0}\sin^2 2\varphi^{(j)}\right)^{1/n}, \tag{27}$$

where $R^{(j)}$ is the half facet width of facet j, and $\varphi^{(j)}$ is the angle between facet j and one of the principal stress directions. The summation extends over all grain boundary facets in the polycrystal. The extension of the slip line estimate, f^{sl}, in (25) to a random polycrystal, however, cannot be done in a unique manner as the grain boundary facets are no longer co-linear. Therefore, we only confine attention to f^{sc}. Figure 9 gives the correlation with the numerical results of f. It is clear that the scatter of the shear crack parameter is too high to speak of a meaningful correlation with the finite element results. Reducing the creep exponent n to 1 does not improve the results as it did for the single grain model (see Figs 6(c) and 6(d)).

Numerous alternatives to such physically motivated estimates of f as the above types have been confronted with the numerical results. However, we have not been able to find one that is capable of capturing the microstructure dependence of the stress enhancement factor. Therefore, we simply introduce an empirical parameter, ρ. This nondimensional parameter is defined per grain as

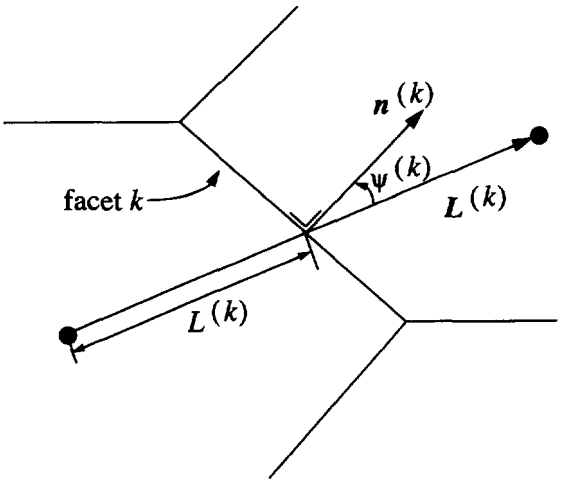

Fig. 10. Definition of quantities $L^{(k)}$ and $\psi^{(k)}$ appearing in definition (28) for the geometrical parameter ρ.

$$\rho = \frac{1}{KA_G} \sum_{k=1}^{K} L^{(k)^2}(1+\sin 2\psi^{(k)}), \tag{28}$$

where K is the number of grain boundary facets of the grain and A_G is the grain area. If $\mathbf{L}^{(k)}$ is the vector connecting the centroids of the grain adjacent to facet k, then $L^{(k)}$ is the length of the part of $\mathbf{L}^{(k)}$ associated with the grain (see Fig. 10). Furthermore, $\psi^{(k)}$ is the angle between $\mathbf{L}^{(k)}$ and the normal $\mathbf{n}^{(k)}$ to facet k. To characterize the entire polycrystal, we just take the average over all grains, $\bar{\rho}$. For a polycrystal built up of regular hexagonal grains, definition (28) reduces to $\rho = \bar{\rho} = 0.289$. It is noted that in the definition of ρ use has been made of the fact that any introduction of randomness increases the stress enhancement factor for the random realizations analyzed here. As a consequence, ρ does not correlate with the results of the single grain model (Fig. 6).

Figure 11 shows the same numerical results as Fig. 9, but now plotted against the geometrical parameter $\bar{\rho}$. The filled symbols correspond to the three microstructures of Fig. 7. The curve is a fit to the results and is described by

$$f = f_0 + 15(\bar{\rho} - \bar{\rho}_0)^2, \tag{29}$$

where $f_0 = 1.198$ and $\bar{\rho}_0 = 0.289$ are the stress enhancement factor and the geometrical parameter for the regular hexagonal polycrystal, respectively. Note that this fit may be slightly dependent on the mesh in view of the observed mesh dependence of f (cf. Section 5.1). This has been checked for three cases, where the number of elements was increased by a factor 1.5. We again found an increasing mesh sensitivity with increasing f, but the differences did not exceed 1.6%.

To investigate the dependence on the creep exponent n, we picked 20 cases from the random Voronoi realizations (type 1) and repeated the calculations for $n = 1, 3, 7$ and 10. Figure 12 shows the results for different n, together with quadratic fits of the results according to

$$f(n, \bar{\rho}) = f_0^n + \tfrac{3}{4}(n+15)(\bar{\rho} - \bar{\rho}_0)^2, \tag{30}$$

where f_0^n is the stress enhancement factor of the regular hexagonal geometry for a creep exponent n. For $n = 5$, this expression reduces to (29). Note that by proposing (30) we implicitly assume that the 20 picked Voronoi cases are representative for all 52 realizations considered.

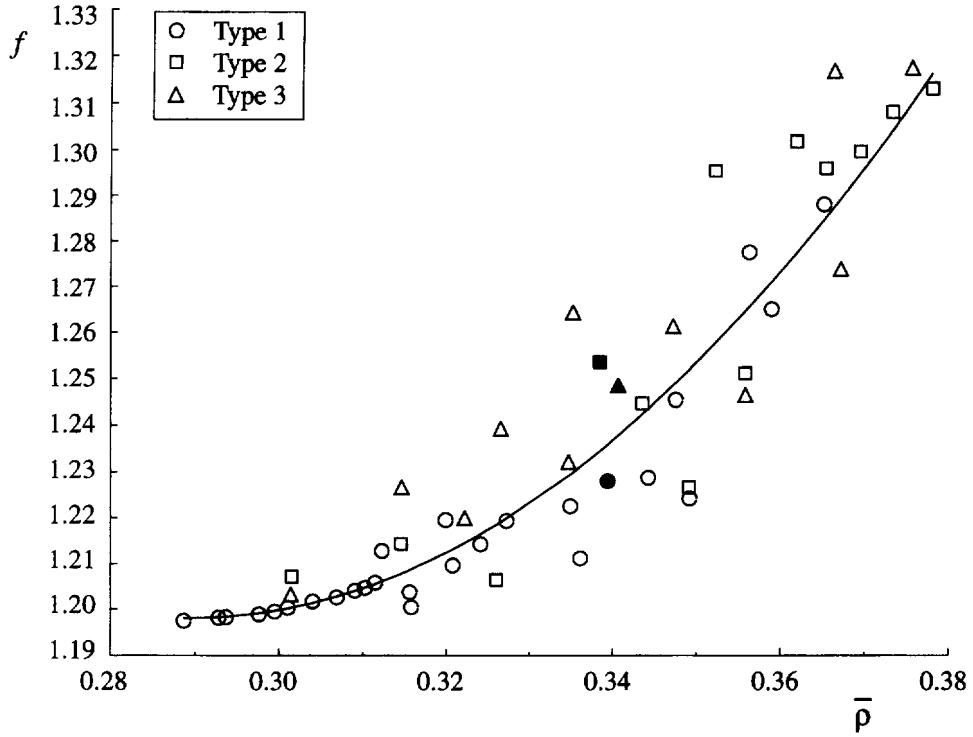

Fig. 11. Correlation of $\bar{\rho}$ with the same finite element results as in Fig. 9. The curve is a quadratic fit according to (29). The filled symbols correspond to the three microstructures of Fig. 7.

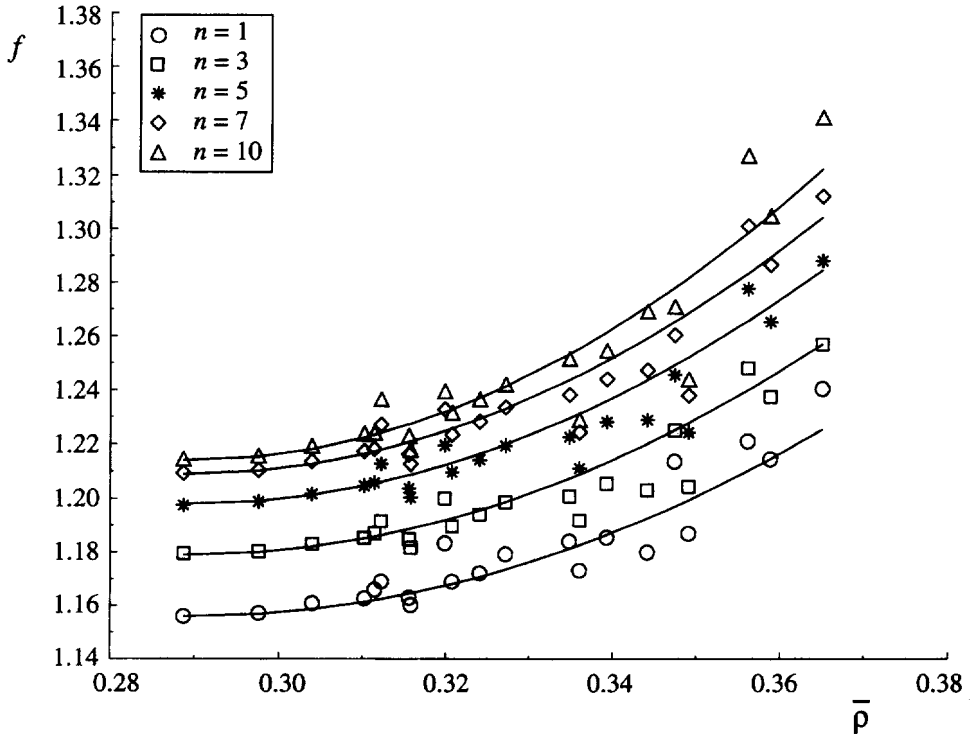

Fig. 12. Finite element results for f against the geometrical parameter $\bar{\rho}$ for different values of the creep exponent n. For each value of n a quadratic fit is shown according to (30).

6. FACET STRESSES

Rodin (1995) has investigated 2-D as well as 3-D disordered arrays of grains corresponding to a Voronoi tessellation of a random point lattice. Without recourse to the governing field equations inside the grains, he obtained an approximate expression for the

principal facet stress, i.e., the facet stress averaged over all facets normal to the maximum principal stress direction. The 2-D analogue predicts that the principal facet stress is the same as for the regular hexagonal microstructure. In this section, we impose random variations on the regular hexagonal structure and compute the implications on the distribution of facet stresses as well as on the principal facet stress.

In analyzing the facet stresses, we simply use the finite element results of the preceding section for a creep exponent $n = 5$. To show the influence of random variations on the distribution of facet stresses, we picked three cases which are generated by varying the Voronoi nuclei (type 1). Figure 13 shows histograms of the facet stresses, normalized by the applied stress Σ_2. Since a one-to-one relation exists between the random realizations and the regular microstructure, we can keep track of the facets which were transverse in the regular microstructure. In the histograms they correspond to the filled bars. From Fig. 13(a) we learn that even a small deviation from the regular hexagonal structure increases the stress considerably on some transverse facets. As the randomness increases, in Figs 13(b) and 13(c), the distribution becomes more uniform, corresponding with higher tensile and compressive stresses on transverse and inclined facets, respectively. It should be noted that, by virtue of the unit cell symmetries, some transverse facets are forced to remain transverse. This is expected to influence the facet stresses slightly.

In contrast to the single grain microstructure, the aggregates in the irregular (8, 8) unit cell microstructures are no longer statically determinate (cf. Section 4), so that a dependence of the facet stresses on the constitution of the grains is to be expected. To investigate this, calculations for the three cases of Fig. 13 have been repeated with creep exponent $n = 1$ and $n = 10$, showing identical results for the facet stresses as compared with $n = 5$. This indicates that the structures analyzed here are approximately statically determinate, and, therefore, we neglect the n-dependence altogether. In 3-D, however, Dib and Rodin (1993) did observe a dependence on n for the principal facet stress, implying that a 3-D aggregate of completely regular grains is statically indeterminate. This may be due to the fact that in 3-D more geometrical constraints are active than in 2-D (Anderson and Rice, 1985).

To further quantify the observations from Fig. 13, we take the average over all transverse facets as an approximation for the principal facet stress in the sense of Rodin (1995). This value is calculated for all cases and shows an increase with randomness. To capture the geometrical variation, we recall that for the single grain model of Fig. 3 under uniaxial tension in the x_2-direction the principal facet stress is given by (23)

$$\sigma_F = \frac{A_0}{2R_0}\Sigma_2, \tag{31}$$

while the inclined facets are stress free. The factor $A_0/2R_0$ in this expression brings about a net-section-stress effect for the single grain model (recall that $A_0/2R_0 = 1.5$ for the regular hexagonal grain). This effect is controlled by the ratio $(A_0 - R_0)/R_0$ (cf. Fig. 3); or, in other words, by the ratio D/B of the length D of the diagonal of the grain that is most transverse to the maximum principal stress direction, and the length B of the parallel grain boundary facet. For irregular hexagonal shapes, the parameter can be defined per half grain by using the projection of the facet on the diagonal for B. Let this geometrical parameter be denoted by μ; as the parameter for the whole polycrystal we just take the average, $\bar{\mu}$. Figure 14 shows the results for all cases, where again the different symbols correspond to the three different types of microstructures described in Section 5.2. The line denotes the linear regression of the results and can be described by

$$\sigma_F = [1.5 + 0.34(\bar{\mu} - \bar{\mu}_0)]\Sigma_2, \tag{32}$$

where $\bar{\mu}_0 = 2$ is the value for the regular hexagonal structure. Note that the same expression holds for the single grain model, but with the factor 0.34 being replaced with 0.5.

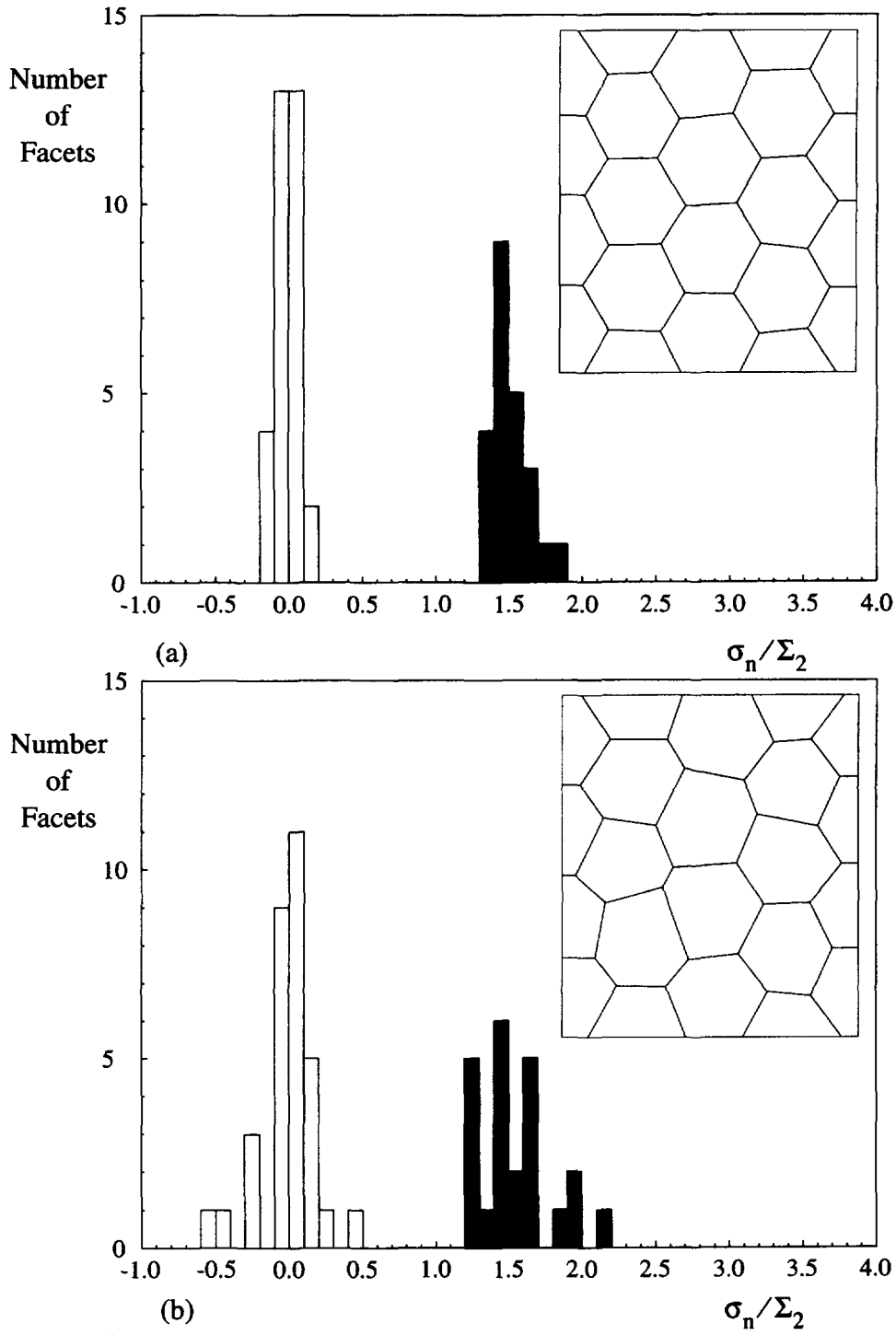

Fig. 13. Histograms of the normalized facet stresses, σ_n/Σ_2, for three microstructures of type 1 and with $n = 5$.

7. CONCLUSION

The effect of variations in microstructure on the overall creep strain rate and facet stresses is studied in planar polycrystalline model materials, consisting of freely sliding grains. It is shown that free sliding renders the material to be highly sensitive to microstructural variations, which results in (i) an increase of the stress enhancement factor f to characterize the enhanced macroscopic creep rate due to sliding, and (ii) an increase in the principal facet stress. Geometrical parameters are proposed that seem to capture the relevant geometrical characteristics responsible for the two phenomena.

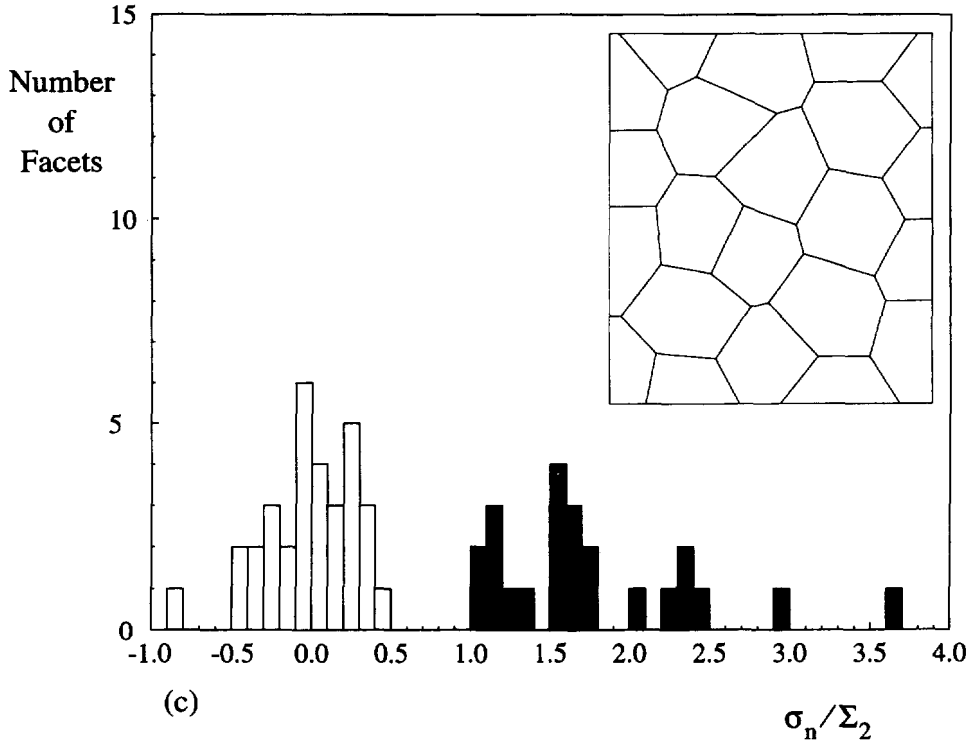

Fig. 13. *Continued.*

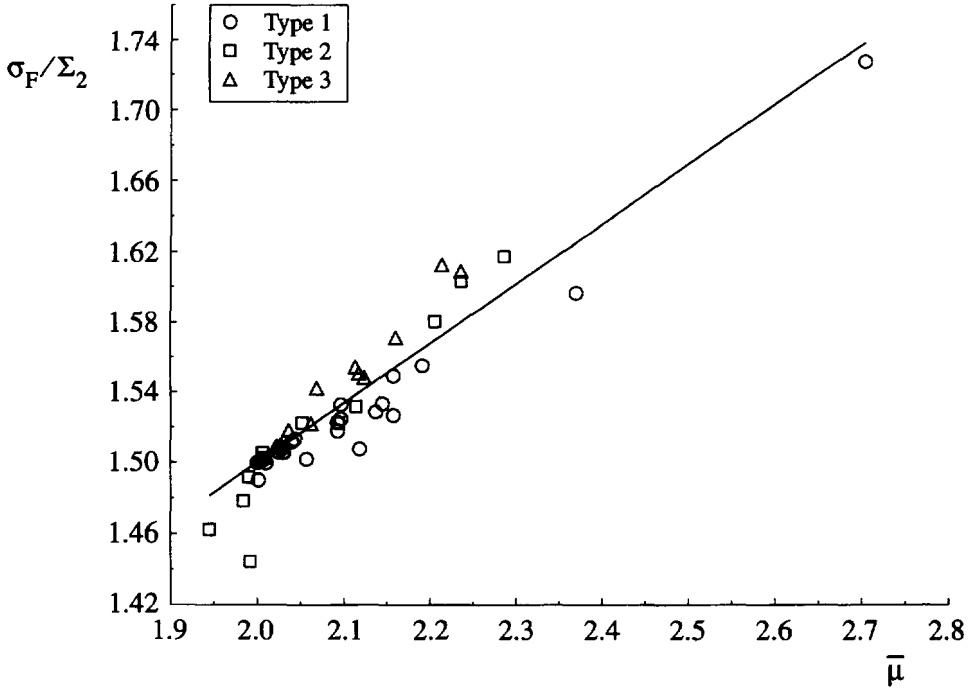

Fig. 14. Normalized principal facet stress, σ_F/Σ_2, against the geometrical parameter $\bar{\mu}$ derived from the same finite element calculations as shown in Figs 9 and 11. The line shows the linear regression according to (32).

In general, the response of aggregates of creeping grains in the presence of grain boundary sliding is anisotropic. For a certain class of aggregates the anisotropy can be described in terms of a fourth-order tensor of which 15 coefficients are independent. This number reduces to 3 in the case of planar polycrystals, so that there are also 3 independent stress enhancement factors. Furthermore, when the material is orthotropic, only 2 remain

to be determined, namely one stress enhancement factor with respect to uniaxial tension and one with respect to simple shear. This paper has only dealt with the former.

In studying the creep rate enhancement, some key features are brought out by investigating a very small unit cell, representing a polycrystal with identical grains. This single grain model focuses on the explicit influence of the grain shape. It appears that the strain rate enhancement for these kind of aggregates can be attributed to a net-section-stress argument along with a wedge effect.

To incorporate random variations the unit cell is enlarged to $(m_1, m_2) = (8, 8)$. Many random realizations are analyzed, generated by three different types of techniques. Surprisingly, all stress enhancement factors exceed the one for the regular hexagonal structure. Based on this observation a geometrical parameter $\bar{\rho}$ is defined, which seems to be able to capture the microstructural dependence of the stress enhancement factor. Finally, an approximate expression for f is proposed as a function of $\bar{\rho}$ and the creep exponent n. In analyzing the influence of randomness on the facet stresses, we observe that high tensile peak stresses develop on the more or less transverse facets, while facet stresses on some inclined facets become compressive. To capture the transverse facet stress enhancement, an expression is proposed for the principal facet stress as a function of the net-section-stress parameter $\bar{\mu}$.

The present work clearly demonstrates that the enhancement of the creep rate as well as of the principal facet stress are inseparable consequences of free grain boundary sliding. Care should be taken, however, to immediately connect the present results to interpretations of intergranular creep damage in random polycrystals. A distinction has to be made between constrained and unconstrained cavity growth. In the latter case, growth of grain boundary cavities is driven by creep, so that the enhanced creep flow contributes directly to the cavity growth rate, resulting in a shorter lifetime as compared to the regular hexagonal microstructure. When cavities grow predominantly by diffusion, the development of damage on grain boundary facets is constrained by creep of the surrounding grains (Dyson, 1976; Rice, 1981; Tvergaard, 1984). Therefore, in the case of isolated cavitating facets in random polycrystals, the enhanced creep flow will indirectly accelerate cavity growth and thus decrease the rupture time. However, when all facets are prone to cavitation, the creep constraint is less dominant, resulting in early microcracks on small transverse facets. Combined with an enhanced creep flow, this accelerates the rupture process considerably (Onck and Van der Giessen, 1995). Thus, the sensitivity of predicted creep rupture times to microstructural variations observed by Van der Giessen and Tvergaard (1994b) seems to be due not only to the enhanced facet stresses on almost transverse grain boundary facets but also to the reduced macroscopic creep resistance.

Care must also be taken in generalizing the present results to realistic 3-D aggregates, since a 3-D spatially staggered packing of grains with free sliding exhibits a higher level of integrity than in 2-D (Anderson and Rice, 1985). In this context it is noteworthy to point out the inherent different natures of the facet stress enhancement and strain rate enhancement due to grain boundary sliding. The former is related to a reduction in load carrying area and is calculated from *average* normal stresses on grain boundary facets. This justifies approaches based on statics alone or on low-dimensional variational formulations (Anderson and Rice, 1985; Rodin, 1995). The strain rate enhancement, however, is directly related to an enhanced highly nonuniform creep flow in the grains, which necessitates a high-dimensional discretization, like the finite element method. Such calculations have been carried out by Dib and Rodin (1993) for a periodic array of truncated octahedra in 3-D, from which they conclude that the strain rate enhancement in 3-D is similar to that in 2-D. However, in light of the mesh-sensitivity found here in 2-D, their finite element mesh may have been too coarse to pick up the highly nonuniform stress distribution inside the grains, so that their results probably underestimate the actual 3-D creep enhancement.

REFERENCES

Anderson, P. M. and Rice, J. R. (1985). Constrained creep cavitation of grain boundary facets. *Acta Metall.* **33**, 409–422.

Ashby, M. F. (1972). Boundary defects and atomistic aspects of boundary sliding and diffusional creep. *Surface Sci.* **31,** 498–542.
Brunner, H. and Grant, N. J. (1959). Deformation resulting from grain boundary sliding. *Trans. AIME* **215,** 48–56.
Cocks, A. C. F. and Ashby, M. F. (1982). On creep fracture by void growth. *Progr. in Mat. Sci.* **27,** 189–244.
Chen, I. W. and Argon, A. S. (1979). Grain boundary and interphase boundary sliding in power law creep. *Acta Metall.* **27,** 749–754.
Crossman, F. W. and Ashby, M. F. (1975). The non-uniform flow of polycrystals by grain-boundary sliding accommodated by power-law creep. *Acta Metall.* **23,** 425–440.
Dib, M. W. and Rodin, G. J. (1993). Three-dimensional analysis of creeping polycrystals using periodic arrays of truncated octahedra. *J. Mech. Phys. Solids* **41,** 725–747.
Dyson, B. F. (1976). Constraints on diffusional cavity growth rates. *Metal Sci.* **10,** 349–353.
Ghahremani, F. (1980). Effect of grain boundary sliding on steady creep of polycrystals. *Int. J. Solids Struct.* **16,** 847–862.
Hill, R. (1967). The essential structure of constitutive laws for metal composites and polycrystals. *J. Mech. Phys. Solids* **15,** 79–95.
Kachanov, M. (1992). Effective elastic properties of cracked solids: critical review of some basic concepts. *Appl. Mech. Rev.* **45,** 304–335.
Lau, C. W. and Argon, A. S. (1977). Stress concentrations caused by grain boundary sliding in metals undergoing power-law creep. In *Fracture* 1977 (ed. Taplin, D. M. R.), pp. 595–601; University of Waterloo Press, Waterloo, Canada.
Nix, W. D., Earthman, J. C., Eggeler, G. and Ilschner, B. (1989). The principal facet stress as a parameter for predicting creep rupture under multiaxial stresses. *Acta Metall.* **37,** 1067–1077.
Onck, P. R. and Van der Giessen, E. (1995). Computational modeling of creep fracture in large polycrystalline aggregates. In *Computational Methods in Micromechanics* (eds Ostoja-Starzewski, M. and Ghosh, S.), pp. 129–146, ASME, San Francisco.
Ponte Castañeda, P. (1991). The effective mechanical properties of nonlinear isotropic composites. *J. Mech. Phys. Solids* **39,** 45–71.
Rice, J. R. (1981). Constraints on the diffusive cavitation of isolated grain boundary facets in creeping polycrystals. *Acta Metall.* **29,** 675–681.
Riedel, H. (1984). Cavity nucleation at particles on sliding grain boundaries. A shear crack model for grain boundary sliding in creeping polycrystals. *Acta Metall.* **32,** 313–321.
Rodin, G. J. (1995). Stress transmission in polycrystals with frictionless grain boundaries. *J. Appl. Mech.* **62,** 1–6.
Tvergaard, V. (1984). On the creep constrained diffusive cavitation of grain boundary facets. *J. Mech. Phys. Solids* **32,** 373–393.
Van der Giessen, E. and Tvergaard, V. (1994a). Development of final creep failure in polycrystalline aggregates. *Acta Met. Mater.* **42,** 959–973.
Van der Giessen, E. and Tvergaard, V. (1994b). Effect of random variations in microstructure on the development of final creep failure in polycrystalline aggregates. *Modell. Simul. Mater. Sci. Engng* **2,** 721–738.
Van der Giessen, E. and Tvergaard, V. (1994c). Simulations of creep failure in polycrystals with random variations in microstructure and with curved grain boundaries. In *Numerical Predictions of Deformation Processes and the Behaviour of Real Materials* (eds Andersen, S. I. *et al.*), pp. 313–318, Risø, Roskilde, Denmark.

APPENDIX

In this Appendix an approximate expression for the stress enhancement factor for the single grain model (Fig. 3) will be derived, based on Riedel's (1984) shear crack analysis.

As pointed out by Brunner and Grant (1959), the contribution of a single sliding grain boundary, $\dot{\delta}$, to the total elongation rate can be calculated from the relative sliding velocity across the facet, $\dot{u}$, by

$$\dot{\delta} = \frac{1}{W}\int_{w} \dot{u}_s \, \mathrm{d}t,$$

where W is the width of the specimen, w the projection of the grain boundary onto the transverse direction, $\mathrm{d}t$ a length increment in the transverse direction and $\dot{u}_s$ the component of $\dot{u}$ in the tensile direction. Note that for the single grain microstructure, the 'tensile direction' can be identified with the direction of maximum principal stress. Thus, for $\Sigma_2 > \Sigma_1$ this yields

$$\dot{\delta}_2 = \frac{1}{A_0} w \bar{u}_2 = \frac{C_0}{A_0}\bar{u}\cos\varphi \sin\varphi = \frac{C_0}{2A_0}\bar{u}\sin 2\varphi, \tag{33}$$

where $\bar{u}$ is the average relative sliding velocity along the inclined facet and $\bar{u}_2$ the component of $\bar{u}$ in the maximum principal tensile stress direction.

Based on a linearized material law for the grains, Riedel (1984) obtained the following expression for the average relative sliding velocity $\bar{u}$ across an isolated shear crack under plane strain conditions:

$$\bar{u} = \frac{3\pi}{8}\sqrt{na}\frac{\dot{E}_e}{\Sigma_e}\tau^{\infty},$$

where a is the width of the facet, τ^{∞} the resolved shear stress on the grain boundary facet, Σ_e the applied effective stress, defined by $\Sigma_e = \frac{1}{2}\sqrt{3}\,|\Sigma_2 - \Sigma_1|$, and $\dot{E}_e$ the corresponding effective strain rate according to (4). Specializing to the single grain problem we get

$$\bar{u} = \frac{3\pi}{8}\sqrt{\frac{n}{3}} C_0 \dot{E}_e \sin 2\varphi. \tag{34}$$

To derive an expression for the stress enhancement factor, the approximation is made that the total stain rate consists of a uniform part, $\dot{E}^{uni}$, valid in the absence of grain boundaries, and a part due to the presence of grain boundaries, $\dot{E}^{gb}$. For $\Sigma_2 > \Sigma_1$ this yields

$$\dot{E}_2^{tot} = \dot{E}_2^{uni} + \dot{E}^{gb} = \tfrac{1}{2}\sqrt{3}\dot{E}_e + \frac{\dot{\delta}_2}{B_0}. \tag{35}$$

Recalling that $\dot{E}_2^{tot} = f^n \dot{E}_2^{uni}$ and combining (33), (34) and (35) yields

$$f = \left(1 + \frac{\pi}{8}\sqrt{n}\frac{C_0^2}{A_0 B_0}\sin^2 2\varphi\right)^{1/n}. \tag{36}$$

The exercise can also be carried out for a biaxial stress state with $\Sigma_1 > \Sigma_2$. This results in the same expression for f, thus showing that the expression (36) satisfies the demand that $f = f_{11} = f_{22}$ (see Section 2.2).